

## RESEARCH ARTICLE

# PI3K regulates endocytosis after insulin secretion by mediating signaling crosstalk between Arf6 and Rab27a

Mami Yamaoka<sup>1</sup>, Tomomi Ando<sup>1</sup>, Takeshi Terabayashi<sup>1</sup>, Mitsuhiro Okamoto<sup>1</sup>, Masahiro Takei<sup>1</sup>, Tomoki Nishioka<sup>2</sup>, Koza Kaibuchi<sup>2,3</sup>, Kohichi Matsunaga<sup>4</sup>, Ray Ishizaki<sup>4</sup>, Tetsuro Izumi<sup>4</sup>, Ichiro Niki<sup>1</sup>, Toshimasa Ishizaki<sup>1</sup> and Toshihide Kimura<sup>1,\*</sup>

**ABSTRACT**

In secretory cells, endocytosis is coupled to exocytosis to enable proper secretion. Although endocytosis is crucial to maintain cellular homeostasis before and after secretion, knowledge about secretagogue-induced endocytosis in secretory cells is still limited. Here, we searched for proteins that interacted with the Rab27a GTPase-activating protein (GAP) EPI64 (also known as TBC1D10A) and identified the Arf6 guanine-nucleotide-exchange factor (GEF) ARNO (also known as CYTH2) in pancreatic  $\beta$ -cells. We found that the insulin secretagogue glucose promotes phosphatidylinositol (3,4,5)-trisphosphate (PIP<sub>3</sub>) generation through phosphoinositide 3-kinase (PI3K), thereby recruiting ARNO to the intracellular side of the plasma membrane. Peripheral ARNO promotes clathrin assembly through its GEF activity for Arf6 and regulates the early stage of endocytosis. We also found that peripheral ARNO recruits EPI64 to the same area and that the interaction requires glucose-induced endocytosis in pancreatic  $\beta$ -cells. Given that GTP- and GDP-bound Rab27a regulate exocytosis and the late stage of endocytosis, our results indicate that the glucose-induced activation of PI3K plays a pivotal role in exocytosis–endocytosis coupling, and that ARNO and EPI64 regulate endocytosis at distinct stages.

**KEY WORDS:** Endocytosis, Small GTPase, Insulin, Membrane trafficking, Diabetes, Pancreatic  $\beta$ -cells

**INTRODUCTION**

Bidirectional intracellular trafficking is fundamental to maintain cellular homeostasis. In secretory cells, endocytosis is coupled to exocytosis to keep the cell volume constant and to prevent excess accumulation of secretory machinery on the plasma membrane after secretion. Therefore, not only exocytosis but also endocytosis is required for proper secretion. Pancreatic  $\beta$ -cells are typical secretory cells that release insulin in response to increased blood glucose levels, and thereby lower the level of glucose in the blood. Impairment of their secretory activity plays an important role in the pathogenesis of diabetes mellitus (Kahn, 2001; Ashcroft and Rorsman, 2004). Although many efforts have been made to clarify the molecular mechanisms of glucose-induced insulin exocytosis, knowledge about glucose-induced endocytosis is still limited.

Small GTPases are almost ubiquitously expressed in eukaryotic cells and include the Ras, Rho, Rab, Ran, and Sar/Arf superfamilies, which modulate intracellular signaling pathways thereby regulating a wide variety of cellular functions (Takai et al., 2001; Wennerberg et al., 2005). Under unstimulated conditions, these proteins localize in the cytosol as an inactive form in which they are bound to GDP and GDP-dissociation inhibitors (GDIs) (Dirac-Svejstrup et al., 1994; Garrett et al., 1994; Ullrich et al., 1994). Cell stimulation activates guanine-nucleotide-exchange factors (GEFs), and thereby converts GDP-bound small GTPases into the GTP-bound, or active, form (Novick and Zerial, 1997). Generally, only the GTP-bound small GTPase, and not the GDP-bound form, is capable of binding to its specific effectors. Such binding mediates the generation of downstream signals that control specific cellular functions. This signaling is terminated by GTPase-activating proteins (GAPs) (Fukui et al., 1997), which convert GTP-bound GTPases back into the GDP-bound form by enhancing the intrinsic GTPase activity of the small GTPase. Regulation of the localization and function of small GTPases is therefore complex and is mediated by the combination of their specific GDIs, GEFs and GAPs.

Both insulin exocytosis and endocytosis involve the Rab family member small GTPase Rab27a, which is highly expressed in pancreatic  $\beta$ -cells (Izumi, 2007; Kimura and Niki, 2011a,b). GTP-bound Rab27a interacts with GTP-dependent effectors, including exophilin 8 (also known as Slac2-c and MyRIP) (Waselle et al., 2003; Ivarsson et al., 2005; Goehring et al., 2007; Mizuno et al., 2011; Brozzi et al., 2012a,b), granuphilin (also known as Slp4a and SYTL4) (Wang et al., 1999; Torii et al., 2002; Gomi et al., 2005) and exophilin 7 (also known as JFC1, Slp1 and SYTL1) (Wang et al., 2013), under basal conditions. These interactions are important for the transport and tethering of insulin granules. We recently identified coronin 3 (also known as CORO1C) and IQGAP1 as new Rab27a-interacting proteins (Kimura et al., 2008, 2013). In contrast to previously established small GTPase interactors, these proteins selectively form a complex with the GDP-bound, but not with the GTP-bound, Rab27a. We found that these interactions appear to have functional significance. Thus, Rab27a is converted from the GTP- into the GDP-bound form following glucose stimulation. Furthermore, GDP-bound Rab27a is recruited to, and IQGAP1 accumulates in, the vicinity of the plasma membrane. Additionally, the binding of GDP-bound Rab27a to coronin 3 enhances the F-actin bundling activity of coronin 3. This activity of Rab27a modulates the late stage of endocytosis (the stage after scission from the plasma membrane) by regulation of retrograde transport of the internalized secretory membrane (Kimura et al., 2010a,b). Thus, neither coronin 3 nor IQGAP1 regulate Rab27a in a manner similar to GDIs, but are rather GDP-dependent effectors, which act as signaling molecules,

<sup>1</sup>Department of Pharmacology, Oita University Faculty of Medicine, 1-1 Idaigaoka, Hasama, Yufu, Oita 879-5593, Japan. <sup>2</sup>Department of Cell Pharmacology, Graduate School of Medicine, Nagoya University, 65 Tsurumai, Showa, Nagoya, Aichi 466-8550, Japan. <sup>3</sup>JST, CREST, 4-1-8 Honcho, Kawaguchi 332-0012, Japan. <sup>4</sup>Laboratory of Molecular Endocrinology and Metabolism, Department of Molecular Medicine, Institute for Molecular and Cellular Regulation, Gunma University, Maebashi, Gunma 371-8512, Japan.

\*Author for correspondence (t.kimura@oita-u.ac.jp)

thereby regulating endocytosis (Yamaoka et al., 2015). These results suggest that GTP- and GDP-bound Rab27a regulate exocytic and endocytic stages in insulin secretion, respectively (Kimura and Niki, 2011a,b).

EPI64 (also known as TBC1D10A) was originally identified as a protein that interacted with ezrin-radixin-moesin-binding phosphoprotein-50 (EBP50, also known as SLC9A3R1) and that regulates microvillar structure in placental syncytiotrophoblast cells (Reczek and Bretscher, 2001; Hanono et al., 2006). EPI64 also functions as a Rab27a GAP through its Tre-Bud-Cdc16 (TBC) domain (Itoh and Fukuda, 2006; Itoh et al., 2006; Imai et al., 2011). We have recently shown that glucose induces the conversion of GTP-bound Rab27a into its GDP-bound form through EPI64 in pancreatic  $\beta$ -cells (Kimura et al., 2010b). These results indicate that EPI64 acts as a molecular switch that promotes endocytosis instead of exocytosis. However, the question of how glucose regulates EPI64 still remains.

In this study, we identified ARNO (also known as cytohesin 2, CYTH2) a GEF for Arf6, as a new EPI64-interacting protein. We found that phosphatidylinositol (3,4,5)-trisphosphate (PIP<sub>3</sub>) generation by glucose-induced activation of phosphoinositide 3-kinase (PI3K) recruits ARNO to the intracellular side of the plasma membrane, and that peripheral ARNO regulates endocytosis through Arf6-mediated clathrin assembly. We also found that peripheral ARNO recruits EPI64 to the same area, and that the interaction requires glucose-induced endocytosis in pancreatic  $\beta$ -cells. Our results suggest that the insulin secretagogue glucose activates PI3K and induces endocytosis through signaling crosstalk between the Arf6 and Rab27a pathways.

## RESULTS

### Identification of ARNO as an EPI64-interacting protein

To determine the activation mechanism of Rab27a, we searched for EPI64-interacting proteins in extracts of the insulin-secreting pancreatic  $\beta$ -cell line MIN6 using a GST–EPI64 affinity column. A GST column was used as a control. Elution of bound proteins and their subsequent analysis by SDS-PAGE and silver staining identified a protein with a molecular mass of 48,000 Da (p48) that specifically bound to GST–EPI64 and not to GST (Fig. 1A). This p48 protein was identified by mass spectrometric analysis as ARNO, which is a GEF for Arf6 (Frank et al., 1998a; Jayaram et al., 2011). To confirm the results obtained in the proteomic analysis, an immunoblot analysis was performed. ARNO was detected in the eluate from GST–EPI64 but not in the other eluates (Fig. 1B). To determine whether EPI64 forms a complex with ARNO in MIN6 cells, a co-immunoprecipitation assay with MIN6 extracts was performed. This analysis demonstrated that ARNO did indeed co-immunoprecipitate with EPI64 (Fig. 1C). The cellular distribution of EPI64 and ARNO in the mouse pancreas was examined by immunohistochemical analysis (Fig. 1D). Both EPI64 and ARNO were detected in insulin-positive  $\beta$ -cells as well as in other types of cells.

We then examined whether EPI64 and ARNO directly interact by using an *in vitro* binding assay with purified recombinant proteins. MBP–ARNO directly bound GST–EPI64 but not GST alone (Fig. 2A). The binding constant and stoichiometry between EPI64 and ARNO were determined using the same assay. The dissociation constant ( $K_d$ ), as determined by Scatchard analysis, was 1.0  $\mu$ M, and the stoichiometry was 0.3 (Fig. 2B). Next, the protein sites required for the interaction were determined by immunoprecipitating lysates from COS-7 cells expressing various GFP–EPI64 and Flag–ARNO deletion mutants. EPI64 bound ARNO-PH (amino acids 250–400,

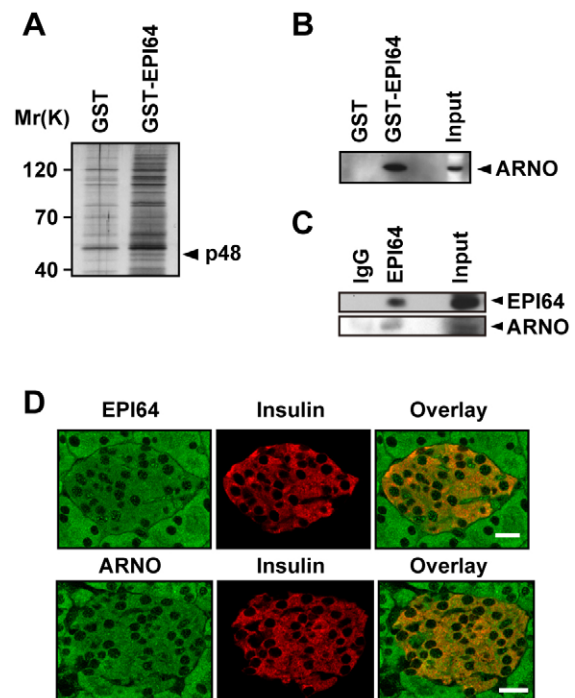


**Fig. 1. Identification of ARNO as an EPI64-interacting protein in pancreatic  $\beta$ -cells.** (A,B) Eluates from affinity columns were analyzed by silver staining (A, the p48 band is indicated) and immunoblotting with anti-ARNO antibody (B). (C) MIN6 extracts were immunoprecipitated with anti-EPI64 antibody. The immunocomplexes were analyzed by immunoblotting with anti-EPI64 or anti-ARNO antibody. (D) Mouse pancreata were double-stained with anti-insulin antibody and anti-EPI64 antibody or anti-ARNO antibody. Scale bars: 20  $\mu$ m.

containing the pleckstrin homology domain) but not Flag or ARNO- $\Delta$ PH (amino acids 1–250) (Fig. 2C). ARNO bound EPI64-C-NT (amino acids 327–420) but not GFP, EPI64- $\Delta$ C (amino acids 1–327) or EPI64-C-CT (amino acids 421–500) (Fig. 2D). The ARNO-binding domain (ABD) of EPI64 differs from the binding sites for other EPI64-interacting proteins (Reczek and Bretscher, 2001; Hokanson and Bretscher, 2012). We confirmed the identified ABD by construction and analysis of the binding of EPI64- $\Delta$ ABD, which specifically lacks ARNO binding activity (Fig. 2D).

### ARNO is required for the glucose-induced translocation of EPI64

We have previously demonstrated that glucose, the most important insulin secretagogue, converts GTP-bound Rab27a into its GDP-bound form through EPI64 (Kimura et al., 2008, 2010b). We therefore examined the effect of glucose on the complex formation between EPI64 and ARNO in MIN6 cells. A co-immunoprecipitation assay showed that stimulation with 20 mM glucose (G20) promoted the interaction between EPI64 and ARNO (Fig. 3A). We next examined the intracellular distribution of EPI64 in glucose-stimulated and unstimulated MIN6 cells. In this experiment, ARNO-silenced MIN6 cells were co-transfected with Flag–EPI64. Immunoblot analysis revealed that ARNO siRNA (siARNO) diminished the expression of endogenous ARNO by 75% without affecting the expression of endogenous EPI64 protein or  $\beta$ -actin (Fig. 3B). EPI64 in control-depleted cells (siControl) was mainly localized in cytosolic vesicles (Fig. 3C,D). Application of 20 mM glucose induced translocation of EPI64 to the vicinity of the plasma membrane. This EPI64 translocation did not occur in ARNO-

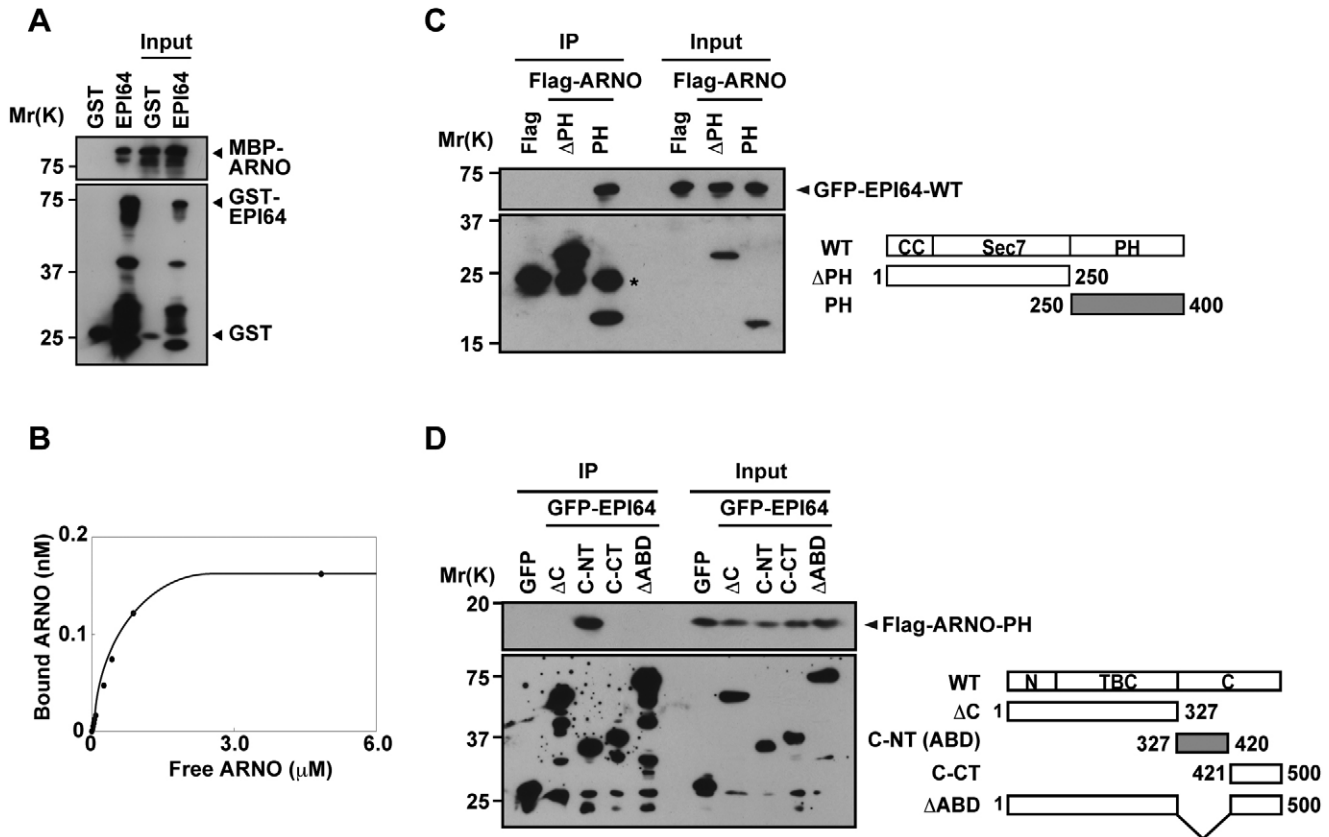


**Fig. 2. ARNO directly binds near the C-terminus of EPI64 through its PH domain.** (A) An *in vitro* binding assay was performed using purified MBP–ARNO and bead-bound GST–EPI64, and immunoblotting of bead-bound proteins was performed with anti-MBP or anti-GST antibody. (B) An *in vitro* binding assay using GST–EPI64 and various concentrations of MBP–ARNO. The dissociation constant was calculated using Scatchard analysis. (C, D) COS-7 extracts expressing constructs of GFP–EPI64 and Flag–ARNO as indicated on the right were immunoprecipitated (IP) with anti-Flag (C) or anti-GFP antibody (D). The immunocomplexes were analyzed by immunoblotting using anti-GFP or anti-Flag antibody. CC, coiled-coil domain; PH, pleckstrin homology domain; N, N-terminus of EPI64; TBC, Tre-2-Bub2-Cdc16 domain; C, C-terminus of EPI64; ABD, ARNO-binding domain. The asterisk indicates the light chain of antibodies.

silenced cells. Co-expression of an siRNA-resistant mutant of ARNO (RNAi<sup>R</sup>-ARNO), with silent point-mutations in the target site of siARNO, could rescue the missorting of EPI64 induced by siARNO. Moreover, EPI64- $\Delta$ ABD did not reproduce the glucose-induced translocation (Fig. 3E, F). These results suggest that ARNO is associated with the translocation of EPI64. EPI64 binds GTP-bound Arf6 (Hanono et al., 2006). Hence, we examined the effect of GTP-bound Arf6 on the translocation of EPI64 to exclude the possibility that EPI64 is recruited to GTP-Arf6, which is produced by ARNO, at the plasma membrane rather than to ARNO itself. Co-expression of RNAi<sup>R</sup>-ARNO-E156K, a catalytically inactive ARNO mutant, could rescue the missorting of EPI64 by siARNO (Fig. 3C, D). Notably, these mutants localized near the plasma membrane where EPI64 accumulated. These results suggest that EPI64 is recruited to ARNO at the plasma membrane rather than to GTP-bound Arf6. We next examined ARNO- and glucose-dependent translocation of EPI64 at the endogenous protein level. Application of 20 mM glucose induced the translocation of endogenous EPI64 to the vicinity of the plasma membrane (Fig. S1A). This translocation did not occur in ARNO-silenced cells. We then examined the effect of that EPI64 siRNA (siEPI64) on the intracellular distribution of ARNO. Immunoblot analysis revealed siEPI64 diminished the expression of endogenous EPI64 by 80% without affecting the expression of endogenous ARNO protein or  $\beta$ -actin (Fig. 3G). ARNO was mainly localized in cytosolic vesicles in glucose-unstimulated cells (Fig. 3H, I). Glucose induced the redistribution of ARNO to the vicinity of the plasma

membrane. The localization of ARNO was not affected in cells in which EPI64 was silenced. These results suggest that ARNO is required for the glucose-induced translocation of EPI64.

We next examined the effect of siARNO on the conversion of Rab27a by pull-down assays (Fig. 3J). Stimulation with 20 mM glucose increased GDP-bound Rab27a without changing the total amount of Rab27a, in agreement with our previous report (Kimura et al., 2008). This increase was inhibited in ARNO-silenced cells. These results suggested that ARNO-dependent translocation of EPI64 is required for the glucose-induced conversion of GTP- into GDP-bound Rab27a.

We next performed time-lapse imaging analysis under total internal reflection fluorescence (TIRF) microscopy to examine the spatial and temporal regulation of endocytic machinery, including EPI64 and ARNO. Glucose stimulation induced a massive brightening, followed by dimming of both clathrin and dynamin 2 puncta just beneath the plasma membrane (Fig. 4A, B), which represents clathrin-dependent endocytosis as previously reported (He et al., 2008). On average, clathrin ( $28.4 \pm 1.0$  s) and dynamin 2 ( $28.9 \pm 1.0$  s) came from the cell interior to the plasma membrane together (mean  $\pm$  s.d., Fig. 4I, J). By contrast, coronin 3 was recruited later than dynamin 2 to the intracellular side of the plasma membrane ( $33.1 \pm 0.9$  and  $28.6 \pm 1.0$  s, respectively;  $P < 0.05$ ) (Fig. 4C, D, I, J). This result is consistent with our previous study, which showed that coronin 3 regulates a late stage of endocytosis, that is, the stage after scission from the

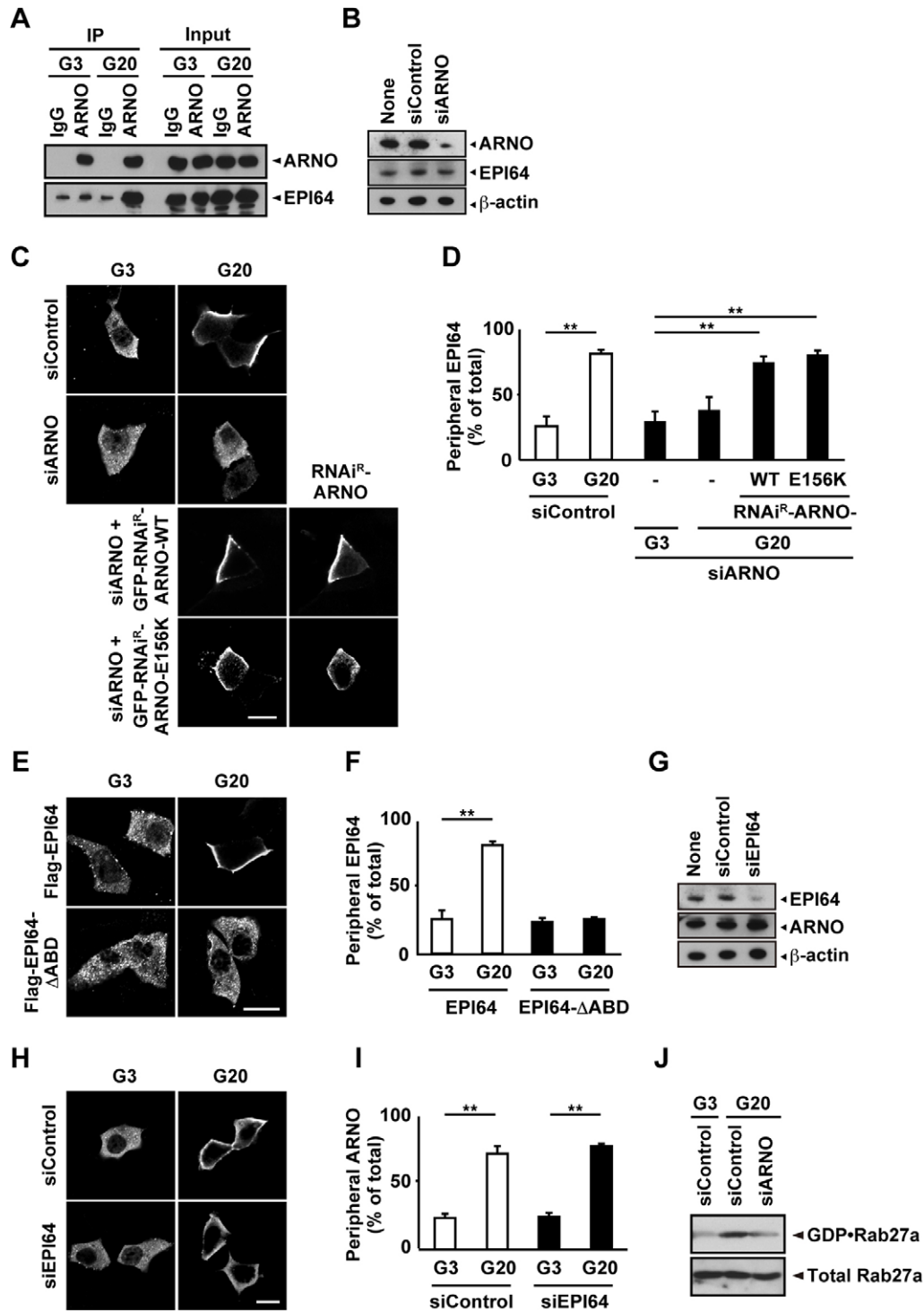


**Fig. 3. ARNO is required for the glucose-induced translocation of EPI64.** (A) MIN6 cells were incubated with 3 or 20 mM glucose (G3 and G20, respectively) for 10 min. The cell extracts were immunoprecipitated (IP) with anti-ARNO antibody. The immunocomplexes were analyzed by immunoblotting with anti-ARNO or anti-EPI64 antibody. (B) ARNO-silenced MIN6 cells were analyzed by immunoblotting with anti-ARNO, anti-EPI64 or anti-β-actin antibody. (C) ARNO-silenced MIN6 cells expressing Flag-EPI64 and GFP-RNAi<sup>R</sup>-ARNO were incubated with 3 or 20 mM glucose for 2 min. The cells were immunostained with anti-Flag antibody. (D) The percentage of cells in C with a peripheral distribution of Flag-EPI64 was analyzed.  $**P < 0.01$  vs G3 (ANOVA, Tukey-Kramer's method). (E) MIN6 cells expressing Flag-EPI64 were incubated with 3 or 20 mM glucose for 2 min. The cells were immunostained with anti-Flag antibody. (F) The percentage of cells in E with a peripheral distribution of Flag-EPI64 was analyzed.  $**P < 0.01$  (Student's *t*-test). (G) EPI64-silenced MIN6 cells were analyzed by immunoblotting with anti-EPI64, anti-ARNO or anti-β-actin antibody. (H) EPI64-silenced MIN6 cells expressing Flag-ARNO were incubated with 3 or 20 mM glucose for 2 min. The cells were immunostained with anti-Flag antibody. (I) The percentage of cells in H with a peripheral distribution of Flag-ARNO was analyzed.  $**P < 0.01$  (Student's *t*-test). (J) MIN6 cells stimulated with 20 mM glucose were extracted and incubated with beads conjugated to GST-coronin-3-ΔC. The bound proteins were analyzed by immunoblotting using anti-Rab27a antibody. Statistical analysis of the percentage of transfected cells that had EPI64 or ARNO near the plasma membrane is shown. More than 40 randomly selected cells (more than 8 cells per experiment) were examined. Data are expressed as means ± s.d. from four independent experiments. Scale bars: 10 μm.

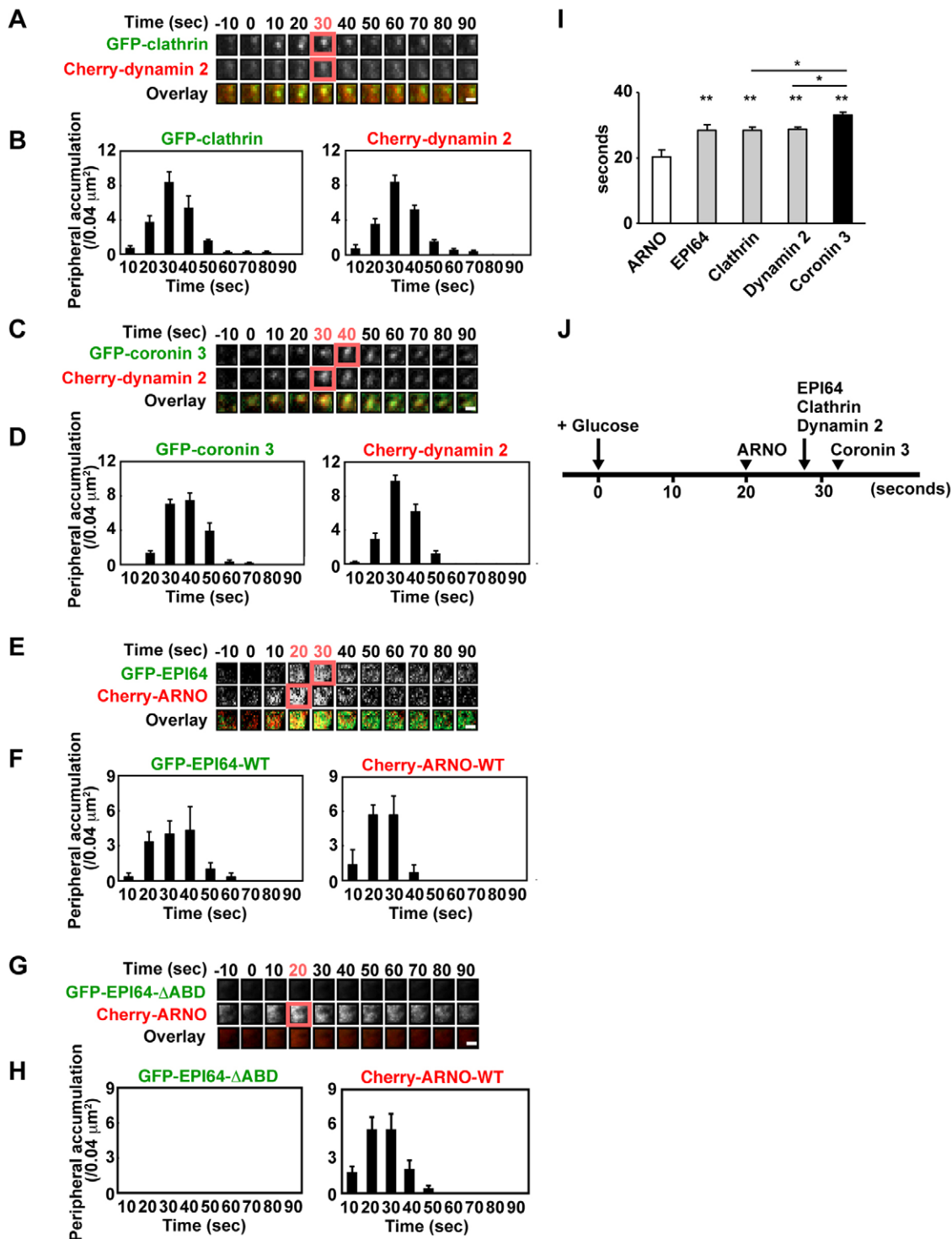


**Fig. 4. ARNO regulates the glucose-induced translocation of EPI64.** (A–H) TIRF images were sampled in living MIN6 cells expressing GFP- and mCherry-tagged proteins. The average fluorescence intensity of individual vesicles was calculated in a  $0.2 \mu\text{m} \times 0.2 \mu\text{m}$  square around the vesicle (A,C,E,G). Peripheral accumulation of fluorescent proteins after 20 mM glucose stimulation was manually counted in each cell (B,D,F,H). (I) The average time during which fluorescent proteins moved from the cell interior to the plasma membrane was plotted. (J) Model depicting accumulation of endocytic proteins just beneath the plasma membrane. More than three randomly selected cells (more than 10 squares per cell) were examined. Data are expressed as means  $\pm$  s.d. from three independent experiments. \* $P < 0.05$ , \*\* $P < 0.01$  (ANOVA, Tukey-Kramer's method). Scale bars:  $0.1 \mu\text{m}$ .

plasma membrane, by modulating the retrograde transport of the internalized membrane, (Kimura et al., 2010b). Consistent with the results of immunostaining (Fig. 3), EPI64 ( $28.4 \pm 1.7$  s) was recruited to the intracellular side of the plasma membrane, where

ARNO accumulated ( $20.3 \pm 2.2$  s,  $P < 0.01$ ; Fig. 4E,F,I,J; Fig. S1B). In contrast, EPI64- $\Delta$ ABD was not recruited to this area (Fig. 4G,H). These results suggest that ARNO regulates the glucose-induced translocation of EPI64.

### PIP<sub>3</sub> generation by glucose-induced activation of PI3K recruits ARNO to the plasma membrane

The activation of ARNO requires the presence of phosphoinositides (Paris et al., 1997). Therefore, we next examined the effect of phosphoinositides on the glucose-induced translocation of ARNO in MIN6 cells. Both wild-type ARNO (ARNO-WT) and ARNO-K268A, which is defective in phosphatidylinositol (4,5)-bisphosphate (PIP<sub>2</sub>) binding, were recruited to the plasma membrane following glucose stimulation, but ARNO-R279C, which is defective in PIP<sub>3</sub> binding, was not (Fig. 5A,B), suggesting that PIP<sub>3</sub> is required for the glucose-induced translocation of ARNO. This result is consistent with a previous report showing that the PH domain of ARNO binds with higher affinity to PIP<sub>3</sub> than to PIP<sub>2</sub> (Macia et al., 2000). To test whether the translocation depends on PI3K activity, we used PI3K inhibitors such as Wortmannin and LY294002. The addition of PI3K inhibitors inhibited the glucose-induced translocation of ARNO-WT (Fig. 5A,B). We next examined endogenous PIP<sub>3</sub> generation by glucose. In this experiment, PIP<sub>3</sub> generation at the plasma membrane was verified using the PH domain as a PIP<sub>3</sub> marker (Macia et al., 2000). Glucose stimulation increased the peripheral distribution of Flag-PH (Fig. 5C,D), suggesting that PIP<sub>3</sub> is generated by glucose in pancreatic  $\beta$ -cells. These results suggest that PIP<sub>3</sub> generation by glucose-induced activation of PI3K recruits ARNO to the plasma membrane.

We next examined whether the activation of PI3K is a direct effect of glucose or an indirect effect mediated through insulin receptors. Neither treatment with insulin nor the potent insulin secretagogue KCl affected the intracellular distribution of ARNO or Flag-PH under these conditions (Fig. 5E–G). Moreover, S961, an insulin receptor antagonist peptide, did not affect glucose-induced translocation of ARNO and Flag-PH (Fig. 5H–J). These results suggest that the activation of PI3K is a direct effect of intracellular glucose signaling rather than an indirect effect mediated by secreted insulin signaling.

### Arf6 GEF activity of peripheral ARNO is essential for glucose-induced clathrin assembly in pancreatic $\beta$ -cells

GTP-bound Arf6 interacts with the clathrin adaptor AP-2 and regulates endocytosis by controlling the assembly of the clathrin coat in HeLa cells (Paleotti et al., 2005). We therefore examined the effect of peripheral ARNO on clathrin assembly in pancreatic  $\beta$ -cells. In this experiment, MIN6 cells expressing GFP-clathrin were visualized by TIRF microscopy. Clathrin fluorescence was seen as distinct puncta on the cell surface (Fig. 6A). Glucose stimulation increased the amount of peripheral clathrin, suggesting that glucose promotes clathrin-dependent endocytosis (Fig. 6A,B). Neither Arf6-Q67L, a GTPase-deficient mutant that mimics the GTP-bound state, nor ARNO-WT affected the glucose-induced increase in the number of peripheral clathrin molecules, probably because endogenous GTP-bound Arf6 and ARNO are sufficient for endocytosis at this period. By contrast, peripheral clathrin was decreased upon the expression of Arf6-T27N, a mutant mimicking GDP-bound Arf6, or ARNO-E156K, which binds and sequesters PIP<sub>3</sub> (Frank et al., 1998b). Peripheral clathrin also decreased in cells expressing ARNO-R279C. Given that ARNO forms a dimer in the cytosol (Chardin et al., 1996), the mutant might bind endogenous ARNO and thereby inhibit ARNO-PIP<sub>3</sub> binding. None of these mutants affected the total amount of clathrin expressed in MIN6 cells (Fig. 6C). We next examined the effect of these mutants on glucose-induced insulin secretion. MIN6 cells expressing Arf6 or ARNO mutants were stimulated with 20 mM glucose for 2 min. The

mutants failed to decrease glucose-induced insulin secretion (Fig. 6D). These results suggest that the mutants do not affect exocytosis under these conditions. This finding is consistent with a previous result showing that ARNO-Arf6 signaling plays an upstream regulatory role for Cdc42, and that the signaling is essential for facilitating second-phase (10–40 min) but not first-phase (<5 min) insulin secretion (Wang et al., 2007; Jayaram et al., 2011). These results suggest that the Arf6 GEF activity of peripheral ARNO is essential for glucose-induced clathrin assembly in pancreatic  $\beta$ -cells.

### The crosstalk between EPI64 and ARNO signaling regulates clathrin-dependent endocytosis

We have demonstrated previously that GDP-bound Rab27a promotes glucose-induced clathrin-dependent endocytosis through its interaction with coronin 3 and IQGAP1 (Kimura et al., 2008, 2013). We therefore examined the effect of the crosstalk between EPI64 and ARNO signaling on endocytosis. In this experiment, internalization of Alexa-Fluor-568-labeled transferrin, a marker of clathrin-dependent endocytosis, was analyzed in ARNO- or EPI64-silenced MIN6 cells. Consistent with our previous study (Kimura et al., 2013), glucose-induced endocytosis resulted in the uptake of transferrin, which showed a punctate pattern in immunofluorescence analysis of control cells (Fig. 7A). Silencing of ARNO using siRNA inhibited the uptake of transferrin compared to control siRNA cells ( $P < 0.01$ ; Fig. 7A,B). Furthermore, co-expression of RNAi<sup>R</sup>-ARNO-WT, but not of the catalytically inactive ARNO mutant RNAi<sup>R</sup>-ARNO-E156K, rescued the inhibition by siARNO ( $P < 0.01$ ). Inhibition of transferrin uptake was also observed in EPI64-silenced cells ( $P < 0.01$ ; Fig. 7A,B). Co-expression of RNAi<sup>R</sup>-EPI64-WT was able to rescue the inhibition by siEPI64 ( $P < 0.01$ ), but that of RNAi<sup>R</sup>-EPI64-R160K, a catalytically inactive EPI64 mutant, or of RNAi<sup>R</sup>-EPI64- $\Delta$ ABD was not. We next performed the same experiments under resting conditions (3 mM glucose). Most of the transferrin was not taken up by endocytosis in control cells (Fig. S2). The same distribution of transferrin was detected in both EPI64- and ARNO-silenced cells, suggesting that the uptake of transferrin is limited under resting conditions and that this uptake is promoted by glucose in pancreatic  $\beta$ -cells. These results suggest that both the Arf6-GEF activity of ARNO and the Rab27a-GAP activity of EPI64 are essential for glucose-induced clathrin-dependent endocytosis. The expression of EPI64-ABD, which is the ARNO-binding site of EPI64 (Fig. 2D), disrupted the interaction between ARNO and EPI64 (Fig. 7C). The uptake of transferrin was inhibited in EPI64-ABD-expressing cells ( $P < 0.01$ ; Fig. 7A,B), suggesting that the interaction between ARNO and EPI64 is essential for glucose-induced clathrin-dependent endocytosis. We further evaluated the effect of this interaction on the endocytosis of secretory membranes by immunofluorescence analysis of the effect of this interaction on the uptake and cellular localization of phogrin (also known as PTPRN2), using antibodies against the phogrin extracellular domain (Vo et al., 2004; Kimura et al., 2010a). It is well established that the integral membrane protein phogrin colocalizes with insulin granules (Pouli et al., 1998) and is taken up by clathrin-dependent endocytosis following glucose-stimulated insulin secretion. Phogrin is then recycled to an insulin-containing compartment and undergoes subsequent rounds of exocytosis (Vo et al., 2004). We obtained similar results to those obtained with the transferrin uptake experiments (Fig. S3A,B), suggesting that the interaction between ARNO and EPI64 is essential for glucose-induced endocytosis of the secretory membrane.

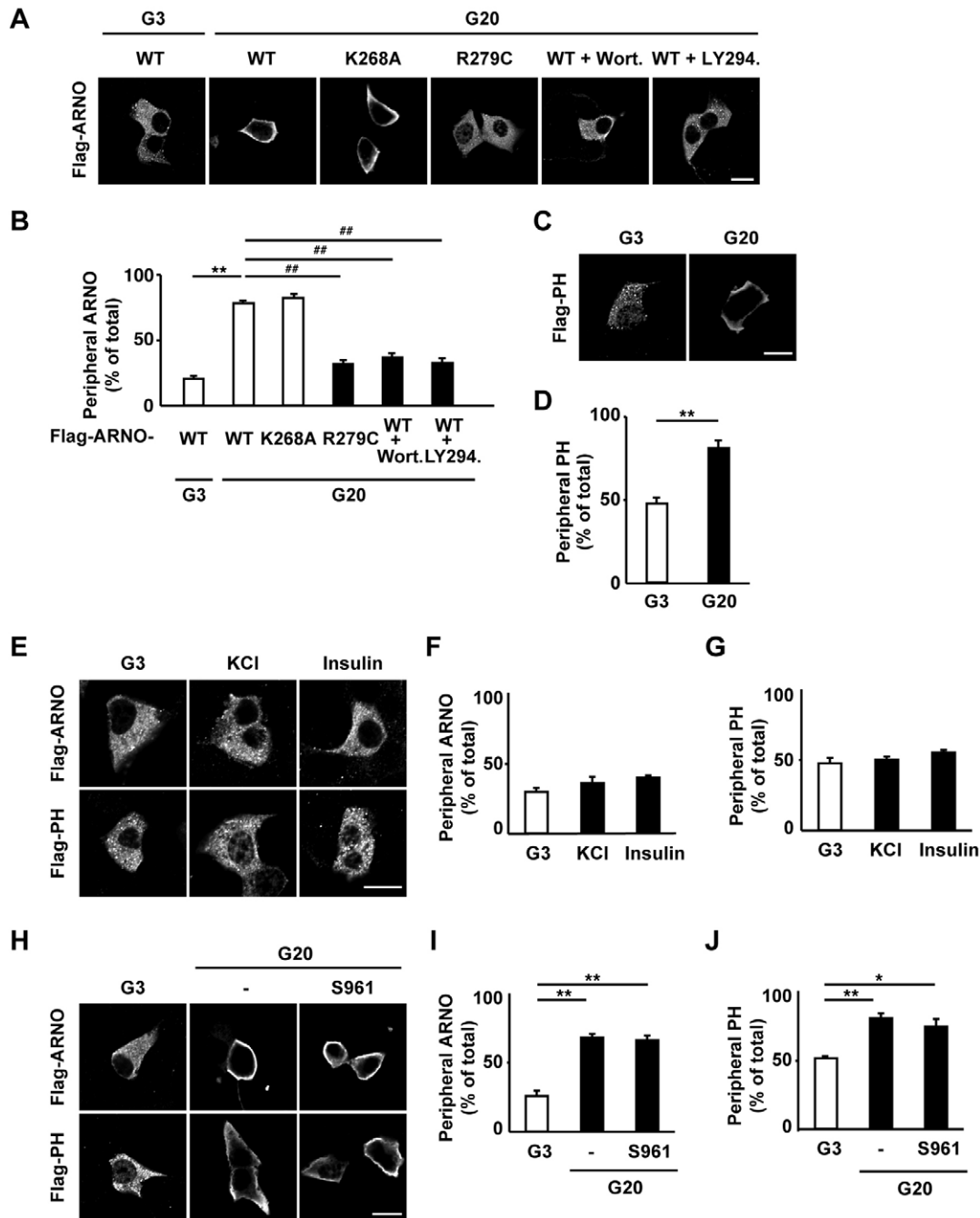


**Fig. 5. PIP<sub>3</sub> generation by glucose-induced activation of PI3K recruits ARNO.** (A) MIN6 cells expressing Flag-ARNO were incubated with 3 or 20 mM glucose (G3 and G20, respectively) for 2 min. The cells were immunostained with anti-Flag antibody. Wort., 100  $\mu$ M Wortmannin; LY294., 50  $\mu$ M LY294002. (B) The percentage of cells in A with a peripheral distribution of Flag-ARNO was analyzed. \*\* $P$ <0.01 vs G3; ## $P$ <0.01 vs G20 (ANOVA, Tukey-Kramer's method). (C) MIN6 cells expressing Flag-PH were incubated with 3 or 20 mM glucose for 2 min. The cells were immunostained with anti-Flag antibody. (D) The percentage of cells in C with a peripheral distribution of Flag-PH was analyzed. \*\* $P$ <0.01 (unpaired Student's  $t$ -test). (E) MIN6 cells expressing Flag-ARNO-WT or Flag-PH were incubated with 50 mM KCl or 100 nM insulin for 2 min. The cells were immunostained with anti-Flag antibody. (F,G) The percentage of cells in E with a peripheral distribution of Flag-ARNO-WT (F) or Flag-PH (G) was analyzed. (H) MIN6 cells expressing Flag-ARNO-WT or Flag-PH were incubated with 100 nM S961 for 2 min. The cells were immunostained with anti-Flag antibody. (I,J) The percentage of cells in H with a peripheral distribution of Flag-ARNO-WT (I) or Flag-PH (J) was analyzed. The statistical significance of differences between means was assessed by. \* $P$ <0.05 vs G3, \*\* $P$ <0.01 vs G3 (ANOVA, Tukey-Kramer's method). More than 40 randomly selected cells (more than 8 cells per experiment) were examined. Data are expressed as means $\pm$ s.d. from four independent experiments. Scale bars: 10  $\mu$ m.

## DISCUSSION

### Glucose-induced endocytosis

In the present study, we clarified the molecular mechanism of glucose-induced endocytosis after insulin secretion (Fig. 8).

Glucose stimulation promotes PI3K activity at the cell periphery, which generates PIP<sub>3</sub> (Figs 5C,D and 8A). The binding of ARNO to this PIP<sub>3</sub> recruits ARNO to the plasma membrane (Fig. 5A,B), where it converts Arf6 from its GDP-bound into its GTP-bound

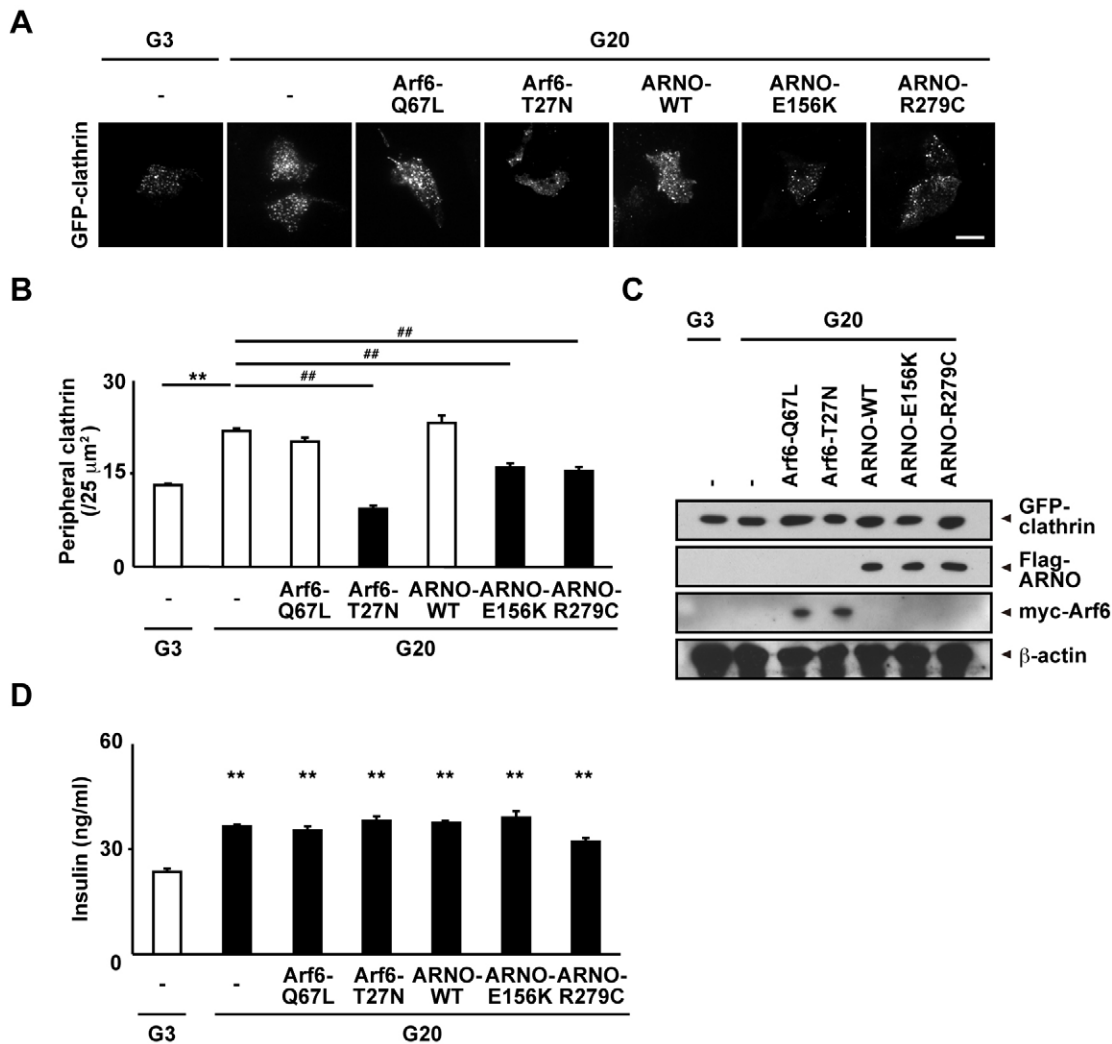


**Fig. 6. Arf6 GEF activity of peripheral ARNO is essential for clathrin assembly in pancreatic  $\beta$ -cells.** (A) TIRF images were sampled in MIN6 cells expressing GFP-clathrin and Myc-Arf6 or Flag-ARNO incubated with 3 or 20 mM glucose (G3 and G20, respectively) for 2 min. (B) Individual vesicles were calculated in a  $5 \mu\text{m} \times 5 \mu\text{m}$  square. More than five randomly selected cells (more than five squares/cell) were examined. Data are expressed as means  $\pm$  s.d. from five independent experiments. \*\* $P < 0.01$  vs G3; ### $P < 0.01$  vs G20 (ANOVA, Tukey-Kramer's method). (C) MIN6 cells expressing GFP-clathrin and Myc-Arf6 or Flag-ARNO incubated with 3 or 20 mM glucose for 2 min were analyzed by immunoblotting with anti-GFP, anti-Flag, anti-Myc or anti- $\beta$ -actin antibody. (D) MIN6 cells expressing Myc-Arf6 or Flag-ARNO were stimulated with 20 mM glucose for 2 min. Insulin contents in the supernatant were determined with an ELISA kit. Data are expressed as means  $\pm$  s.d. from three independent experiments. \*\* $P < 0.01$  vs G3 (ANOVA, Tukey-Kramer's method). Scale bar: 10  $\mu\text{m}$ .

form (Fig. 8B). EPI64 is next recruited to the same area in which ARNO has accumulated (Figs 3C,D, 4, 8B; Fig. S1B). The recruitment of EPI64 might be promoted by conformational changes in ARNO, because  $\text{PIP}_3$  binding promotes the GEF activity of ARNO (Chardin et al., 1996; Venkateswarlu et al., 1998). Peripheral EPI64 converts Rab27a from the GTP- into the GDP-bound form (Kimura et al., 2008). Glucose stimulation also causes increases in intracellular  $\text{Ca}^{2+}$  through ATP-sensitive  $\text{K}^+$  ( $\text{K}_{\text{ATP}}$ )-channel-dependent pathways and promotes fusion between insulin granules and the plasma membrane, resulting in insulin release from pancreatic  $\beta$ -cells (Fig. 8B). GTP-bound Arf6 forms clathrin-coated pits through AP-2 (Figs 4, 6 and 8C). Dynamin 2 is recruited to the neck of the forming vesicle, where it causes scission of the vesicle membrane (Figs 4 and 8D). After scission from the plasma membrane, coronin 3 activity is then required for the retrograde transport of the internalized secretory membrane. The F-actin-bundling activity of coronin 3, and its recruitment to the plasma membrane, are enhanced by its binding to GDP-bound Rab27a

(Kimura et al., 2008, 2010a,b). We therefore consider that EPI64 functions at the late stage of endocytosis through the conversion of GTP-bound Rab27a into the GDP-bound form. Indeed, neither siEPI64 together with RNAi<sup>R</sup>-EPI64- $\Delta$ ABD nor EPI64-ABD affected the dynamics or number of peripheral clathrin molecules (Fig. S4), although these mutants inhibited clathrin-dependent endocytosis (Fig. 7). The same result was observed in cells expressing coronin 3- $\Delta$ C, the dominant-negative coronin 3 that forms an inactive complex with GDP-bound Rab27a. These results suggest that EPI64 regulates the late stage of endocytosis, that is, the stage after the accumulation of clathrin molecules. The present paper demonstrates, for the first time, that glucose-induced activation of PI3K plays a pivotal role in exocytosis–endocytosis coupling, and that ARNO and EPI64 regulate endocytosis at distinct stages.

In the present study, we have shown that glucose regulates the early stage of endocytosis through GTP-bound Arf6 and the late stage through GDP-bound Rab27a. In pancreatic  $\beta$ -cells, the effect

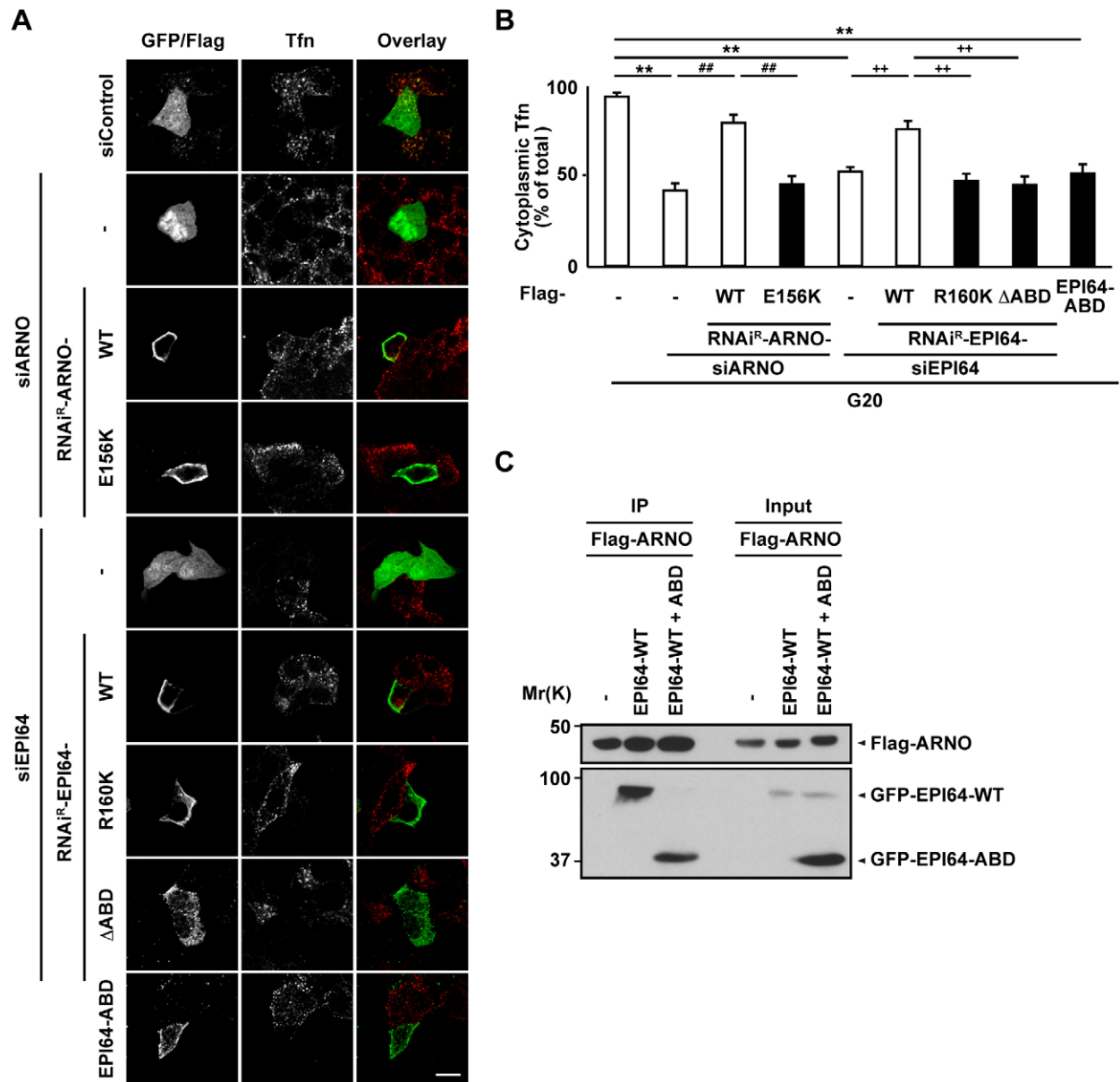


**Fig. 7. The crosstalk between EPI64 and ARNO signaling regulates clathrin-dependent endocytosis.** (A) ARNO- or EPI64-silenced MIN6 cells expressing GFP, Flag-ARNO or Flag-EPI64 were incubated with Alexa-568-labeled transferrin (red) in the presence of 20 mM glucose for 5 min followed by immunofluorescence analysis. (B) The percentage of transfected cells that showed a cytoplasmic distribution of Alexa-Fluor-568-labeled transferrin was analyzed. More than 40 randomly selected cells (more than 8 cells per experiment) were examined. Data are expressed as means±s.d. from four independent experiments. \*\* $P < 0.01$  vs control siRNA; ## $P < 0.01$  vs RNAi<sup>R</sup>-ARNO-WT, ++ $P < 0.01$  vs RNAi<sup>R</sup>-EPI64-WT (ANOVA, Tukey-Kramer's method). (C) COS-7 extracts expressing Flag-ARNO, GFP-EPI64, and GFP-EPI64-ABD were immunoprecipitated (IP) with anti-Flag antibody. The immunocomplexes were analyzed by immunoblotting using anti-Flag or anti-GFP antibody. Scale bar: 10  $\mu$ m.

of GTP-bound Arf6 involves its regulation of the conversion of the Rho family protein Cdc42, from the GDP- to the GTP-bound form, which has a number of cellular functions (Wang et al., 2007; Jayaram et al., 2011). One function is activation of the Rho family member Rac1 through p21-activating kinase (Wang et al., 2007). A second function is the regulation of the dissociation of exocysts and the subsequent formation of endocytic machinery by binding to peripheral IQGAP1. The modulated endocytic machinery includes GDP-bound Rab27a and its effector protein coronin 3 (Rittmeyer et al., 2008; Kimura et al., 2013). Therefore, glucose-induced signaling regulates membrane trafficking by influencing the activity of each small GTPase in direct and indirect feedback processes.

### Glucose-sensing mechanisms

In order to maintain proper blood glucose levels, it is essential that glucose-induced insulin secretion is regulated. In pancreatic  $\beta$ -cells, insulin secretion is promoted through both  $K_{ATP}$ -channel-dependent and -independent pathways following glucose transportation into the cells through the glucose transporter. In response to glucose metabolism,  $K_{ATP}$  channels close, which results in the activation of voltage-dependent  $Ca^{2+}$  channels and a subsequent increase in intracellular  $Ca^{2+}$ , which promotes fusion of the membranes of insulin granules with the plasma membrane (Seino and Miki, 2003). Although many findings regarding the  $K_{ATP}$ -channel-dependent pathway have been reported, knowledge

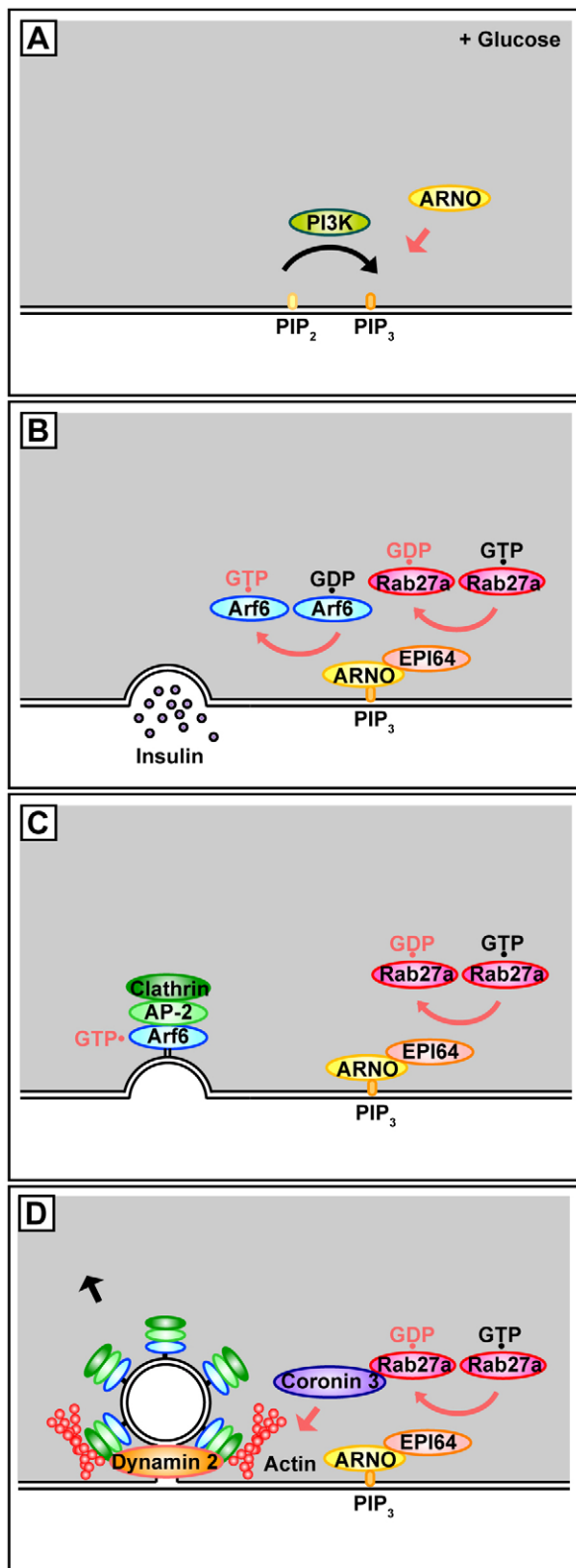


**Fig. 8. A model for glucose-induced endocytosis.** (A) Glucose stimulation activates peripheral PI3K, leading to PIP<sub>3</sub> generation. PIP<sub>3</sub> recruits ARNO to the plasma membrane. (B) EPI64 is recruited to the area where ARNO has accumulated. Peripheral ARNO converts GDP-bound Arf6 into its GTP-bound form. Peripheral EPI64 converts Rab27a from the GTP- into the GDP-bound form. Glucose stimulation also causes increases in intracellular Ca<sup>2+</sup> through ATP-sensitive K<sup>+</sup> (K<sub>ATP</sub>)-channel-dependent pathways and promotes fusion between insulin granules and the plasma membrane, resulting in insulin release from pancreatic  $\beta$ -cells. (C) GTP-bound Arf6 forms clathrin-coated pits through AP-2. (D) Dynamin 2 is recruited at the neck of the forming vesicle and induces vesicle membrane scission. GDP-bound Rab27a recruits its binding protein coronin 3 to the plasma membrane and promotes the F-actin-bundling activity of coronin 3, which is necessary for endocytosis at the late stage after scission.

found that glucose, but not KCl, induces a specific decrease in insulin secretion from the islets of ashen mice with a natural-occurring mutation in Rab27a (Kasai et al., 2005) and converted the GDP-bound form of both Cdc42 and its downstream Rac1 into their GTP-bound forms (Wang et al., 2007). Given that these small GTPases regulate exocytosis and endocytosis, we consider that the K<sub>ATP</sub>-channel-independent pathway is partly involved in the regulation of membrane trafficking.

Both Cdc42 and Rac1 are converted from the GDP- into the GTP-bound forms by D-glucose, but not by L-glucose (a non-transportable glucose analog), 2-deoxyglucose (a non-metabolizable glucose analog) or 3-orthomethylglucose (another non-metabolizable glucose analog) (Wang et al., 2007). This is consistent with our previous results showing that neither L-glucose nor 2-deoxyglucose stimulation recruits Rab27a from the cytosol to the plasma membrane, where IQGAP1 has accumulated (Kimura et al., 2013). These results suggest that the pathway is selective for D-glucose.

In the present study, we have shown that the glucose-induced activation of PI3K is not an indirect effect of the insulin receptor. This finding is consistent with a previous report showing that a slight, but clear, signal of peripheral GFP-PH fluorescence is detectable before the increase in intracellular Ca<sup>2+</sup> when MIN6 cells are stimulated with D-glucose (Hagren and Tengholm, 2006). This observation raises the possibility that pancreatic  $\beta$ -cells have another glucose-sensing mechanism that promotes insulin secretion in cooperation with the K<sub>ATP</sub>-channel-dependent pathway. Further studies are required to investigate the regulation of PI3K by D-glucose in pancreatic  $\beta$ -cells.

### Endocytosis and diabetes mellitus

The impairment of insulin secretion leads to the onset of type 2 diabetes mellitus (Kahn, 2001; Ashcroft and Rorsman, 2004). In the present study, we elucidated the molecular mechanisms of glucose-induced endocytosis. Given that endocytosis is a fundamental step for another round of insulin exocytosis, the process might be involved in the pathogenesis of diabetes. Indeed, some molecules concerning endocytic pathways are associated with insulin secretion and diabetes mellitus. Both ashen mice and mice lacking PI3K show glucose intolerance with decreased insulin secretion (Kasai et al., 2005; Kaneko et al., 2010). The silencing of ARNO or Arf6 inhibits glucose-induced second-phase insulin secretion (Jayaram et al., 2011). Glucose-induced second-phase insulin secretion is also decreased in cells expressing ARNO-E156K or Arf6-T27N. Diabetes increases oxidative stress, which can downregulate PI3K, leading to a decrease in PIP<sub>3</sub>. Indeed, PIP<sub>3</sub> levels are decreased in the livers of type 2 diabetic rats (Manna and Jain, 2012). The same results are expected in pancreatic  $\beta$ -cells, because

about the K<sub>ATP</sub>-channel-independent pathway is still limited (Gembal et al., 1992; Sato et al., 1992; Henquin, 2000; Aizawa et al., 2002). The involvement of K<sub>ATP</sub>-channel-dependent and -independent pathways in insulin secretion have been investigated by comparison of the effect of glucose with that of KCl, which mimics K<sub>ATP</sub>-channel-dependent insulin secretion. It has been

the cells are sensitive to oxidative stress. Taken together, the elucidation of the endocytic pathway might lead to the isolation of therapeutic targets for type 2 diabetes mellitus.

## MATERIALS AND METHODS

### Materials

pAcGFP and pmCherry were purchased from Takara (Shiga, Japan). pcDNA3.1/Hygro(-), pGEX-4T-1 and pMAL-p4x were purchased from Life Technologies (Paisley, UK), GE Healthcare (Buckinghamshire, UK), and New England BioLabs (Hertfordshire, UK), respectively. The following antibodies were used: monoclonal anti-ARNO (sc-59451; 1:200) and anti-GFP (sc-9996; 1:200) antibodies (Santa Cruz Biotechnology, Santa Cruz, CA); polyclonal anti-MBP (E8030S; 1:1000) antibody (New England BioLabs); polyclonal anti-GFP antibody (MBL, Aichi, Japan; 1:200); polyclonal anti-Flag antibody (Thermo Scientific, Bonn, Germany; 1:200); monoclonal anti-Flag (M2), anti- $\beta$ -actin (AC-15; 1:500), and monoclonal anti-GST (GST-2; 1:500) antibodies (Sigma-Aldrich, St Louis, MO); polyclonal anti-insulin antibody (Dako, Carpinteria, CA; 1:50); and monoclonal anti-myc (9E10) antibody (Covance, Princeton, NJ; 1:200). For antibody production, New Zealand White rabbits (Kyudo, Saga, Japan) were immunized with a synthetic peptide corresponding to the C-terminal amino acids of EPI64 (amino acids 483–500) and ARNO (amino acids 387–400), and both antibodies were affinity-purified by exposure to antigen-bound Affigel 102 beads (Bio-Rad, Hercules, CA) and were used at 1:200. S961 and insulin were obtained from Sigma-Aldrich and Eli Lilly (Indianapolis, IN), respectively. COS-7 cells were obtained from the Cell Resource Center for Biomedical Research, Tohoku University. The insulin-secreting  $\beta$ -cell line MIN6 was kindly provided by Jun-Ichi Miyazaki (Osaka University, Japan). Other materials and chemicals were obtained from commercial sources. This study was approved by the Ethical Committee for Animal Experiments at Oita University.

### Plasmid constructs

pcDNA-Flag was generated as described previously (Kimura et al., 2008). cDNAs encoding coronin 3 were obtained as described previously (Kimura et al., 2008). cDNAs of mouse Arf6, ARNO, clathrin light chain  $\alpha$ , dynamin 2, EPI64 and ARNO were amplified by polymerase chain reaction (PCR) from a MIN6 cDNA library. The cDNAs encoding ARNO-PH, ARNO- $\Delta$ PH, EPI64- $\Delta$ C, -C-NT, -C-CT, and  $\Delta$ ABD were also amplified by PCR. All the DNA point mutations were introduced using the Quikchange kit (Agilent Technologies, Santa Clara, CA). siRNA-resistant mutants were created by introducing three silent mutations into ARNO (5'-CCAA-TGAAGGCAGCAAGACATTGCA-3') and EPI64 (5'-GGAGAGCGAG-GATACCTATTGTAA-3') (the underlines indicate mutations).

### Cell culture and transfection

COS7 and MIN6 cells were cultured in Dulbecco's modified Eagle's medium (Sigma-Aldrich) supplemented with 10% and 15% fetal bovine serum, respectively. Lipofectamine 2000 (Life Technologies) reagents were used for transfection according to the manufacturer's instructions.

### Protein purification

GST and MBP fusion proteins were purified according to the manufacturer's protocol. The proteins were then dialyzed against TED buffer [20 mM Tris-HCl pH 7.5, 1 mM ethylene diaminetetraacetic acid (EDTA) and 1 mM dithiothreitol (DTT)].

### EPI64 affinity column chromatography

GST or GST-EPI64 at a concentration of 2  $\mu$ M was incubated with 250  $\mu$ l of glutathione-Sepharose-4B beads (GE Healthcare) for 1 h at 4°C under rotation. After packing the beads into columns, MIN6 cell cytosolic fractions were loaded onto the prepared columns and washed with TED buffer. The proteins bound to the affinity columns were eluted with TED buffer containing 1.5 M NaCl. Proteins in the eluates were separated by SDS-PAGE and detected by the Silver Quest staining kit (Life Technologies). The bands were analyzed by liquid chromatography tandem mass spectrometry (LC-MS/MS) as described previously

(Nishioka et al., 2012). The eluates were also subjected to immunoblotting with monoclonal anti-ARNO antibody.

### Co-immunoprecipitation assay

Immunoprecipitation was performed as described previously (Kimura et al., 2013). In brief, MIN6 cells were extracted by the addition of L1 buffer [20 mM Tris-HCl pH 7.5, 100 mM NaCl, 1 mM EDTA, 50  $\mu$ g/ml phenylmethylsulfonyl fluoride (PMSF), 10  $\mu$ g/ml leupeptin, 10  $\mu$ g/ml aprotinin and 0.1% NP-40] and were incubated with polyclonal anti-EPI64 or monoclonal anti-ARNO antibody. The immunocomplex was then precipitated with protein A or G Sepharose 4B (GE Healthcare). The bound proteins were subjected to immunoblotting with monoclonal anti-ARNO or anti-EPI64 antibody. For this blot, 0.7% of the total lysate was loaded as input.

### Binding assay

Immunoprecipitation was performed as described previously (Kimura et al., 2013). In brief, COS-7 cells expressing GFP-EPI64 and Flag-ARNO mutants were solubilized with L2 buffer (20 mM Tris-HCl pH 7.5, 100 mM NaCl, 1 mM EDTA, 50  $\mu$ g/ml PMSF, 10  $\mu$ g/ml leupeptin, 10  $\mu$ g/ml aprotinin, and 0.1% NP-40). GFP-EPI64 or Flag-ARNO was immunoprecipitated with polyclonal anti-GFP or monoclonal anti-Flag antibody. The immunocomplex was subjected to immunoblotting with monoclonal anti-GFP or polyclonal anti-Flag antibody. For this blot, 0.7% of the total was loaded as input. For the direct binding assay using purified recombinant proteins, glutathione-Sepharose-4B beads coated with GST or GST-EPI64 were incubated with MBP-ARNO in TED buffer at 4°C for 1 h. The beads were then washed with TED buffer and resuspended with SDS-PAGE sampling buffer. The bound proteins were subjected to immunoblotting with anti-GST or anti-MBP antibody.

### Pulldown assay

Pulldown assays were performed as described previously (Kimura et al., 2008). In brief, MIN6 cells, pre-incubated with HEPES-buffered Krebs buffer (20 mM HEPES pH 7.4, 119 mM NaCl, 4.8 mM KCl, 2.5 mM CaCl<sub>2</sub>, 1.2 mM MgSO<sub>4</sub>, 1.2 mM KH<sub>2</sub>PO<sub>4</sub>, 5 mM NaHCO<sub>3</sub> and 1 mg/ml BSA) with 3 mM glucose were incubated with the same buffer with 20 mM glucose for 1 min at 37°C. Proteins were solubilized with L3 buffer (50 mM Tris-HCl pH 7.4, 30 mM MgCl<sub>2</sub>, 10% glycerol, 100 mM NaCl, 1 mM DTT, 1  $\mu$ M PMSF, 10  $\mu$ g/ml leupeptin, 10  $\mu$ g/ml aprotinin and 0.5% Triton X-100) at 4°C for 5 min followed by centrifugation at 14,000 g for 5 min. The supernatants were then incubated with GST-coronin-3- $\Delta$ C-conjugated glutathione-Sepharose 4B beads at 4°C for 1 h. The beads were then washed with L3 buffer and resuspended with SDS-PAGE sampling buffer. The bound proteins were subjected to immunoblotting with anti-Rab27a antibody.

### Immunohistochemistry

Pancreata from male ICR mice (SLC, Shizuoka, Japan), aged 10 weeks, were fixed with phosphate-buffered 3% paraformaldehyde and cryosectioned at a thickness of 5  $\mu$ m. The tissue sections were subjected to immunostaining. Cryosections of the fixed pancreata were incubated with a mixture of anti-insulin antibody and polyclonal anti-EPI64 antibody or polyclonal anti-ARNO antibody, followed by incubation with a mixture of Alexa-568- and Alexa-488-conjugated second antibodies (Life Technologies). All animal experiments were performed according to approved guidelines.

### siRNA preparation

EPI64 (MSS235491)- and ARNO (MSS237639)-specific siRNAs were purchased from Life Technologies. NegaConNaito1 (RNAi Co., Ltd., Tokyo, Japan) was used as a negative control.

### Immunofluorescence analyses

Immunofluorescence analyses were performed as described previously (Kimura et al., 2013). In brief, MIN6 cells expressing GFP- or Flag-tagged proteins were pre-incubated with HEPES-buffered Krebs buffer with 3 mM

glucose followed by incubation with the same buffer with 20 mM glucose, or 20 mM glucose with 100 nM S961, 50 mM KCl or 100 nM insulin. The cells were then rinsed in phosphate-buffered saline, fixed with 4% paraformaldehyde, permeabilized with 0.3% Triton X-100 and stained with anti-Flag antibody, followed by Alexa-Fluor-568-conjugated second antibody. We traced the intracellular fluorescence signals and performed statistical analyses as described previously (Kimura et al., 2013). Cells with obvious peaks in the vicinity of the plasma membrane were counted. We defined the vicinity of the plasma membrane as the outermost 10% of the cell area (Kuroda and Fukuda, 2004). For immunofluorescence analysis of endogenous proteins, the same assay was performed using anti-EPI64 antibody as a primary antibody. For transferrin-uptake experiments, MIN6 cells were incubated in HEPES-buffered Krebs buffer with 20 mM glucose and 5 µg/ml Alexa-Fluor-568-labeled transferrin for 5 min. The cells were then thoroughly washed with phosphate-buffered saline and fixed with 4% paraformaldehyde. For analysis of transferrin uptake, the percentage of cells with a cytoplasmic pattern of staining of these molecules was evaluated (Kimura et al., 2013).

#### Uptake of Alexa-Fluor-568-labeled anti-phogrin antibody

Uptake experiments of anti-phogrin antibody were performed as described previously (Kimura et al., 2010a). In brief, MIN6 cells were incubated for 15 min at 37°C in medium containing anti-phogrin antibody that was labeled with Alexa Fluor 568 using Zenon technology (Thermo Scientific). At the end of the incubation, the cells were washed with phosphate-buffered saline and fixed with 4% paraformaldehyde.

#### Confocal fluorescence microscopy

Images illustrated were acquired using a 100× oil objective (Plan-Apochromat 100×/1.46 Oil DIC; Carl Zeiss, Oberkochen, Germany). All sections were analyzed using a confocal laser microscopy system and software (LSM710; Carl Zeiss) that was built around an inverted microscope (Axio Observer Z1; Carl Zeiss).

#### Total internal reflection fluorescence microscopy

TIRF microscopy was performed as described previously (Wang et al., 2013). Images illustrated were acquired using a 100× oil objective (CFI Apo TIRF 100×/1.49 Oil DIC; Nikon, Tokyo, Japan). All images were analyzed using a TIRF microscopy system and software (NIS-Element; Nikon) that was built around an inverted microscope (ECLIPSE Ti-E; Nikon). Under TIRF microscopy, MIN6 cells expressing GFP- and mCherry-tagged proteins were pre-incubated with HEPES-buffered Krebs buffer with 3 mM glucose at 37°C. Stimulation was achieved by the addition of the same volume of HEPES-buffered Krebs buffer with 40 mM glucose, resulting in a final concentration of 20 mM glucose. The average fluorescence intensity of individual vesicles was calculated in a 0.2 µm×0.2 µm square around the vesicle by NIS-Element.

#### Insulin content

MIN6 cells ( $2 \times 10^6$ ) expressing Myc- or Flag-tagged proteins were pre-incubated with HEPES-buffered Krebs buffer with 3 mM glucose followed by incubation with the same buffer with 20 mM glucose for 2 min. Insulin content in the supernatant was determined using a mouse insulin ELISA kit (Shibayagi, Gunma, Japan) according to the manufacturer's instructions.

#### Statistical analysis

All data are expressed as means±s.d. Data were evaluated for statistical significance using the unpaired Student's *t*-test. Where appropriate, differences were tested by ANOVA followed by Tukey-Kramer's method.

#### Acknowledgements

We thank Dr Jun-Ichi Miyazaki (Osaka University) for providing the MIN6 cells. We also thank Ms Saemi Himeno, Ms Yumi Mizoguchi, Mr Takanori Aoki and Dr Shigeki Taniguchi (Oita University) for the preparation of some materials, and Ms Kaori Tasaka for technical assistance.

#### Competing interests

The authors declare no competing or financial interests.

#### Author contributions

M.Y. designed and performed experiments and wrote the article. T.A., T.T., M.O. and M.T. performed experiments. T.N. and K.K. contributed to the mass analysis. K.M., R.I. and T.I. supervised and interpreted TIRF experiments. I.N. and T.I. performed experiments. T.K. designed and performed experiments and wrote the article.

#### Funding

This research was supported by KAKENHI grants [grant numbers 19790636, 21790876, 23791039 and 26461342]; the Takeda Science Foundation; Novo Nordisk Pharma; Oita Broadcasting System Cultural Foundation; the Suzuken Memorial Foundation; and the joint research program of the Institute for Molecular and Cellular Regulation, Gunma University [grant number 11028].

#### Supplementary information

Supplementary information available online at <http://jcs.biologists.org/lookup/suppl/doi:10.1242/jcs.180141/-/DC1>

#### References

- Aizawa, T., Sato, Y. and Komatsu, M. (2002). Importance of nonionic signals for glucose-induced biphasic insulin secretion. *Diabetes* **51** Suppl. 1, S96–S98.
- Ashcroft, F. M. and Rorsman, P. (2004). Molecular defects in insulin secretion in type-2 diabetes. *Rev. Endocr. Metab. Disord.* **5**, 135–142.
- Brozzi, F., Lajus, S., Diraison, F., Rajatileka, S., Hayward, K., Regazzi, R., Molnar, E. and Varadi, A. (2012a). MyRIP interaction with MyoVa on secretory granules is controlled by the cAMP-PKA pathway. *Mol. Biol. Cell* **23**, 4444–4455.
- Brozzi, F., Diraison, F., Lajus, S., Rajatileka, S., Philips, T., Regazzi, R., Fukuda, M., Verkade, P., Molnar, E. and Varadi, A. (2012b). Molecular mechanism of myosin Va recruitment to dense core secretory granules. *Traffic* **13**, 54–69.
- Chardin, P., Paris, S., Antonny, B., Robineau, S., Beraud-Dufour, S., Jackson, C. L. and Chabre, M. (1996). A human exchange factor for ARF contains Sec7- and pleckstrin-homology domains. *Nature* **384**, 481–484.
- Dirac-Svejstrup, A. B., Soldati, T., Shapiro, A. D. and Pfeffer, S. R. (1994). Rab-GDI presents functional Rab9 to the intracellular transport machinery and contributes selectivity to Rab9 membrane recruitment. *J. Biol. Chem.* **269**, 15427–15430.
- Frank, S., Upender, S., Hansen, S. H. and Casanova, J. E. (1998a). ARNO is a guanine nucleotide exchange factor for ADP-ribosylation factor 6. *J. Biol. Chem.* **273**, 23–27.
- Frank, S. R., Hatfield, J. C. and Casanova, J. E. (1998b). Remodeling of the actin cytoskeleton is coordinately regulated by protein kinase C and the ADP-ribosylation factor nucleotide exchange factor ARNO. *Mol. Biol. Cell* **9**, 3133–3146.
- Fukui, K., Sasaki, T., Imazumi, K., Matsuura, Y., Nakanishi, H. and Takai, Y. (1997). Isolation and characterization of a GTPase activating protein specific for the Rab3 subfamily of small G proteins. *J. Biol. Chem.* **272**, 4655–4658.
- Garrett, M. D., Zahner, J. E., Cheney, C. M. and Novick, P. J. (1994). GDI1 encodes a GDP dissociation inhibitor that plays an essential role in the yeast secretory pathway. *EMBO J.* **13**, 1718–1728.
- Gembal, M., Gilon, P. and Henquin, J. C. (1992). Evidence that glucose can control insulin release independently from its action on ATP-sensitive K<sup>+</sup> channels in mouse B cells. *J. Clin. Invest.* **89**, 1288–1295.
- Goehring, A. S., Pedroja, B. S., Hinke, S. A., Langeberg, L. K. and Scott, J. D. (2007). MyRIP anchors protein kinase A to the exocyst complex. *J. Biol. Chem.* **282**, 33155–33167.
- Gomi, H., Mizutani, S., Kasai, K., Itoharu, S. and Izumi, T. (2005). Granuphilin molecularly docks insulin granules to the fusion machinery. *J. Cell Biol.* **171**, 99–109.
- Hagren, O. I. and Tengholm, A. (2006). Glucose and insulin synergistically activate phosphatidylinositol 3-kinase to trigger oscillations of phosphatidylinositol 3,4,5-trisphosphate in beta-cells. *J. Biol. Chem.* **281**, 39121–39127.
- Hanono, A., Garbett, D., Reczek, D., Chambers, D. N. and Bretscher, A. (2006). EPI64 regulates microvillar subdomains and structure. *J. Cell Biol.* **175**, 803–813.
- He, Z., Fan, J., Kang, L., Lu, J., Xue, Y., Xu, P., Xu, T. and Chen, L. (2008). Ca<sup>2+</sup> triggers a novel clathrin-independent but actin-dependent fast endocytosis in pancreatic beta cells. *Traffic* **9**, 910–923.
- Henquin, J. C. (2000). Triggering and amplifying pathways of regulation of insulin secretion by glucose. *Diabetes* **49**, 1751–1760.
- Hokanson, D. E. and Bretscher, A. P. (2012). EPI64 interacts with Slp1/JFC1 to coordinate Rab8a and Arf6 membrane trafficking. *Mol. Biol. Cell* **23**, 701–715.
- Imai, A., Yoshie, S., Ishibashi, K., Haga-Tsujimura, M., Nashida, T., Shimomura, H. and Fukuda, M. (2011). EPI64 protein functions as a physiological GTPase-activating protein for Rab27 protein and regulates amylase release in rat parotid acinar cells. *J. Biol. Chem.* **286**, 33854–33862.
- Itoh, T. and Fukuda, M. (2006). Identification of EPI64 as a GTPase-activating protein specific for Rab27A. *J. Biol. Chem.* **281**, 31823–31831.
- Itoh, T., Satoh, M., Kanno, E. and Fukuda, M. (2006). Screening for target Rabs of TBC (Tre-2/Bub2/Cdc16) domain-containing proteins based on their Rab-binding activity. *Genes Cells* **11**, 1023–1037.

- Ivarsson, R., Jing, X., Waselle, L., Regazzi, R. and Renstrom, E. (2005). Myosin 5a controls insulin granule recruitment during late-phase secretion. *Traffic* **6**, 1027-1035.
- Izumi, T. (2007). Physiological roles of Rab27 effectors in regulated exocytosis. *Endocr. J.* **54**, 649-657.
- Jayaram, B., Syed, I., Kyathanahalli, C. N., Rhodes, C. J. and Kowluru, A. (2011). Arf nucleotide binding site opener [ARNO] promotes sequential activation of Arf6, Cdc42 and Rac1 and insulin secretion in INS 832/13 beta-cells and rat islets. *Biochem. Pharmacol.* **81**, 1016-1027.
- Kahn, S. E. (2001). Clinical review 135: the importance of beta-cell failure in the development and progression of type 2 diabetes. *J. Clin. Endocrinol. Metab.* **86**, 4047-4058.
- Kaneko, K., Ueki, K., Takahashi, N., Hashimoto, S., Okamoto, M., Awazawa, M., Okazaki, Y., Ohsugi, M., Inabe, K., Umehara, T. et al. (2010). Class IA phosphatidylinositol 3-kinase in pancreatic beta cells controls insulin secretion by multiple mechanisms. *Cell Metab.* **12**, 619-632.
- Kasai, K., Ohara-Imaizumi, M., Takahashi, N., Mizutani, S., Zhao, S., Kikuta, T., Kasai, H., Nagamatsu, S., Gomi, H. and Izumi, T. (2005). Rab27a mediates the tight docking of insulin granules onto the plasma membrane during glucose stimulation. *J. Clin. Invest.* **115**, 388-396.
- Kimura, T. and Niki, I. (2011a). Rab27a in pancreatic beta-cells, a busy protein in membrane trafficking. *Prog. Biophys. Mol. Biol.* **107**, 219-223.
- Kimura, T. and Niki, I. (2011b). Rab27a, actin and beta-cell endocytosis. *Endocr. J.* **58**, 1-6.
- Kimura, T., Kaneko, Y., Yamada, S., Ishihara, H., Senda, T., Iwamatsu, A. and Niki, I. (2008). The GDP-dependent Rab27a effector coronin 3 controls endocytosis of secretory membrane in insulin-secreting cell lines. *J. Cell Sci.* **121**, 3092-3098.
- Kimura, T., Taniguchi, S. and Niki, I. (2010a). Actin assembly controlled by GDP-Rab27a is essential for endocytosis of the insulin secretory membrane. *Arch. Biochem. Biophys.* **496**, 33-37.
- Kimura, T., Taniguchi, S., Toya, K. and Niki, I. (2010b). Glucose-induced translocation of coronin 3 regulates the retrograde transport of the secretory membrane in the pancreatic beta-cells. *Biochem. Biophys. Res. Commun.* **395**, 318-323.
- Kimura, T., Yamaoka, M., Taniguchi, S., Okamoto, M., Takei, M., Ando, T., Iwamatsu, A., Watanabe, T., Kaibuchi, K., Ishizaki, T. et al. (2013). Activated Cdc42-bound IQGAP1 determines the cellular endocytic site. *Mol. Cell Biol.* **33**, 4834-4843.
- Kuroda, T. S. and Fukuda, M. (2004). Rab27A-binding protein Slp2-a is required for peripheral melanosome distribution and elongated cell shape in melanocytes. *Nat. Cell Biol.* **6**, 1195-1203.
- Macia, E., Paris, S. and Chabre, M. (2000). Binding of the PH and polybasic C-terminal domains of ARNO to phosphoinositides and to acidic lipids. *Biochemistry* **39**, 5893-5901.
- Manna, P. and Jain, S. K. (2012). Decreased hepatic phosphatidylinositol-3,4,5-triphosphate (PIP3) levels and impaired glucose homeostasis in type 1 and type 2 diabetic rats. *Cell. Physiol. Biochem.* **30**, 1363-1370.
- Mizuno, K., Ramalho, J. S. and Izumi, T. (2011). Exophilin8 transiently clusters insulin granules at the actin-rich cell cortex prior to exocytosis. *Mol. Biol. Cell* **22**, 1716-1726.
- Nishioka, T., Nakayama, M., Amano, M. and Kaibuchi, K. (2012). Proteomic screening for Rho-kinase substrates by combining kinase and phosphatase inhibitors with 14-3-3zeta affinity chromatography. *Cell Struct. Funct.* **37**, 39-48.
- Novick, P. and Zerial, M. (1997). The diversity of Rab proteins in vesicle transport. *Curr. Opin. Cell Biol.* **9**, 496-504.
- Paleotti, O., Macia, E., Luton, F., Klein, S., Partisani, M., Chardin, P., Kirchhausen, T. and Franco, M. (2005). The small G-protein Arf6GTP recruits the AP-2 adaptor complex to membranes. *J. Biol. Chem.* **280**, 21661-21666.
- Paris, S., Beraud-Dufour, S., Robineau, S., Bigay, J., Antonny, B., Chabre, M. and Chardin, P. (1997). Role of protein-phospholipid interactions in the activation of ARF1 by the guanine nucleotide exchange factor Arno. *J. Biol. Chem.* **272**, 22221-22226.
- Pouli, A. E., Emmanouilidou, E., Zhao, C., Wasmeier, C., Hutton, J. C. and Rutter, G. A. (1998). Secretory-granule dynamics visualized in vivo with a phogrin-green fluorescent protein chimera. *Biochem. J.* **333**, 193-199.
- Reczek, D. and Bretscher, A. (2001). Identification of EPI64, a TBC/rabGAP domain-containing microvillar protein that binds to the first PDZ domain of EBP50 and E3KARP. *J. Cell Biol.* **153**, 191-206.
- Rittmeyer, E. N., Daniel, S., Hsu, S.-C. and Osman, M. A. (2008). A dual role for IQGAP1 in regulating exocytosis. *J. Cell Sci.* **121**, 391-403.
- Sato, Y., Aizawa, T., Komatsu, M., Okada, N. and Yamada, T. (1992). Dual functional role of membrane depolarization/Ca<sup>2+</sup> influx in rat pancreatic B-cell. *Diabetes* **41**, 438-443.
- Seino, S. and Miki, T. (2003). Physiological and pathophysiological roles of ATP-sensitive K<sup>+</sup> channels. *Prog. Biophys. Mol. Biol.* **81**, 133-176.
- Takai, Y., Sasaki, T. and Matozaki, T. (2001). Small GTP-binding proteins. *Physiol. Rev.* **81**, 153-208.
- Torii, S., Zhao, S., Yi, Z., Takeuchi, T. and Izumi, T. (2002). Granuphilin modulates the exocytosis of secretory granules through interaction with syntaxin 1a. *Mol. Cell Biol.* **22**, 5518-5526.
- Ullrich, O., Horiuchi, H., Bucci, C. and Zerial, M. (1994). Membrane association of Rab5 mediated by GDP-dissociation inhibitor and accompanied by GDP/GTP exchange. *Nature* **368**, 157-160.
- Venkateswarlu, K., Oatey, P. B., Tavare, J. M. and Cullen, P. J. (1998). Insulin-dependent translocation of ARNO to the plasma membrane of adipocytes requires phosphatidylinositol 3-kinase. *Curr. Biol.* **8**, 463-466.
- Vo, Y. P., Hutton, J. C. and Angleson, J. K. (2004). Recycling of the dense-core vesicle membrane protein phogrin in Min6 beta-cells. *Biochem. Biophys. Res. Commun.* **324**, 1004-1010.
- Wang, J., Takeuchi, T., Yokota, H. and Izumi, T. (1999). Novel rabphilin-3-like protein associates with insulin-containing granules in pancreatic beta cells. *J. Biol. Chem.* **274**, 28542-28548.
- Wang, Z., Oh, E. and Thurmond, D. C. (2007). Glucose-stimulated Cdc42 signaling is essential for the second phase of insulin secretion. *J. Biol. Chem.* **282**, 9536-9546.
- Wang, H., Ishizaki, R., Xu, J., Kasai, K., Kobayashi, E., Gomi, H. and Izumi, T. (2013). The Rab27a effector exophilin7 promotes fusion of secretory granules that have not been docked to the plasma membrane. *Mol. Biol. Cell* **24**, 319-330.
- Waselle, L., Coppola, T., Fukuda, M., Iezzi, M., El-Amraoui, A., Petit, C. and Regazzi, R. (2003). Involvement of the Rab27 binding protein Slac2c/MyRIP in insulin exocytosis. *Mol. Biol. Cell* **14**, 4103-4113.
- Wennerberg, K., Rossman, K. L. and Der, C. J. (2005). The Ras superfamily at a glance. *J. Cell Sci.* **118**, 843-846.
- Yamaoka, M., Ishizaki, T. and Kimura, T. (2015). Interplay between Rab27a effectors in pancreatic beta-cells. *World J. Diabetes* **6**, 508-516.

Special Issue on 3D Cell Biology  
Call for papers  
Submission deadline: February 15th, 2016  
Deadline extended  
Journal of Cell Science